

1 Occurrence and source apportionment of perfluoroalkyl acids 2 (PFAAs) in the atmosphere in China

3 Deming Han¹, Yingge Ma², Cheng Huang², Xufeng Zhang¹, Hao Xu¹, Yong Zhou¹, Shan Liang¹,
4 Xiaojia Chen¹, Xiqian Huang¹, Haoxiang Liao¹, Shuang Fu¹, Xue Hu¹, Jinping Cheng¹

5 ¹ School of Environmental Science and Engineering, Shanghai Jiao Tong University, Shanghai 200240, China

6 ² State Environmental Protection Key Laboratory of the Formation and Prevention of Urban Air Pollution Complex,
7 Shanghai Academy of Environmental Sciences, Shanghai 200233, China

8 *Correspondence to:* Jinping Cheng (jpcheng@sjtu.edu.cn)

9 **Abstract:**

10 Perfluoroalkyl acids (PFAAs) are a form of toxic pollutant that can be transported across the globe and accumulated in
11 the bodies of wildlife and humans. A nationwide geographical investigation considering atmospheric PFAAs [via](#)
12 [XAD–Passive Air Sampler](#) was conducted [in 23 different provinces/municipalities/autonomous regions](#) in China, which
13 provides an excellent chance to investigate their occurrences, spatial trends, and potential sources. The total [atmospheric](#)
14 concentrations of thirteen PFAAs ([n=268](#)) were 6.19–292.6 pg/m³, with an average value of 39.8±28.1 pg/m³, which
15 were higher than other urban levels but lower than point source measurements. Perfluorooctanoic acid (PFOA) was the
16 dominant PFAAs (20.6%), followed by perfluoro–hexanoic acid (PFHxA), perfluorooctane sulfonate (PFOS), and
17 perfluoro–heptanoic acid (PFPeA). An increasing seasonal trend of PFAAs concentrations was shown as summer <
18 autumn < spring < winter, which may be initiated by stagnant meteorological conditions. Spatially, the content of PFAAs
19 displayed a declining gradient trend of [central of China> northern of China> eastern of China> northeast of China>](#)
20 [southwest of China> northwest of China> southern of China areas](#), and Henan contributed as the largest proportion of
21 PFAAs. Four sources of PFAAs were identified using a positive matrix factorization (PMF) model, including
22 PFOS–based products (26.1%), PFOA–based, and PFNA–based products (36.6%), degradation products of
23 fluoro–telomere–based products (15.5%), and an unknown source (21.8%).

25 **1.Introduction**

26 Perfluoroalkyl acids (PFAAs) are a class of [ionizable](#) polyfluoroalkyl substances (PFASs), which have excellent
27 characteristics in terms of chemical and thermal stability, high surface activity, and water and oil repulsion (Lindstrom et
28 al., 2011; Wang et al., 2014). They are applied to a wide variety of domestic and industrial products such as textiles, oil

29 and liquid repellents, firefighting foam, pesticides, and food packaging materials (Xie et al., 2013;Wang et al., 2014).
30 PFAAs can be released to the surrounding environment during manufacturing and use of PFAAs containing products,
31 which are ubiquitous in the environment (e.g., in the atmosphere, water, or snow) [\(Dreyer et al., 2009;Wang et al.,](#)
32 [2017;Hu et al., 2016\)](#), in wildlife [\(Sedlak et al., 2017\)](#), and even in the human body [\(Cardenas et al., 2017;Tian et al.,](#)
33 [2018\)](#). PFAAs can change adult thyroid hormone levels, reduce newborn birth weight, and biomagnify in the food chain,
34 which can be extremely toxic to animals and humans (Hu et al., 2016;Jian et al., 2017;Baard Ingegerdsson et al., 2010).
35 Of the PFAAs, the long-chain ($C \geq 7$) perfluoroalkyl carboxylic acids (PFCAs) and ($C \geq 6$) perfluoroalkyl sulfonic acids
36 (PFSAAs) are more toxic and bio-accumulative than their short-chain analogues (Konstantinos et al., 2010). This
37 especially applies to perfluorooctanoic acid (PFOA) and perfluorohexane sulfonate (PFHxS) for which have been
38 regulated in numerous countries, while perfluorooctane sulfonate (PFOS) have been added to Annex B of the Stockholm
39 Convention in 2009 (Johansson et al., 2008).

40 PFAAs can originate from direct sources of products' emissions as well as indirect sources of incomplete degradation of
41 their precursors. It is estimated that the global historical emission quantities of C4–C14 PFCAs were 2610–21400 t in the
42 period of 1951–2015, of which PFOA-based and perfluorononanoic-acid (PFNA)-based products contributed the most
43 (Wang et al., 2014). A trend of geographical distribution of major fluorochemical manufacturing sites has shifted from
44 Western Europe, US, and Japan to the emerging economies in the Asia Pacific area over the past decades. This is
45 especially true for China, which was the world's largest industrial contributor of PFOAs (50–80 t) and PFOS-related
46 compounds (~1800 t) in 2009 (Xie et al., 2013). PFOA- and PFOS- based products were added to the Catalogue for the
47 Guidance of Industrial Structure Adjustment in China in 2011, and restricted elimination of PFOA/PFOS substances
48 production were conducted. With a large quantity of PFAAs and their products manufacturing and consumption, China
49 has become the emerging contamination hotspots in the world. In spite of several studies on atmospheric PFAAs levels
50 having been conducted in a few cities (Liu et al., 2015) and point sources (Yao et al., 2016a;Tian et al., 2018) in China,
51 due to the imbalanced urbanization and industrialization levels, there is still a lack of systemic research on atmospheric
52 PFAAs quantification and trends in China.

53 Additionally, the long range or mesoscale transport was also suggested to have a contribution to PFAAs in the air (Dreyer
54 et al., 2009;Cai et al., 2012a). In general, three pathways/hypotheses for the transportation of PFAAs were suggested:
55 transport associated with particles, degradation from precursor, and sea salts from current bursting in coastal areas. The
56 PFAAs precursors such as fluoro-telomere alcohols (FTOHs), which can form the corresponding PFAAs through
57 oxidation reactions initiated by hydroxyl radicals ($\text{OH}\cdot$) in the atmosphere (Thackray and Selin, 2017), are more volatile
58 than PFAAs and can reach remote areas via long-range transportation (Martin et al., 2006; Wang et al., 2018). Due to the

59 lower acid dissociation coefficient (pK_A), 0–3.8 for PFCAs and –3.3 for PFSAs, PFAAs are expected to be mainly
60 associated with aerosols in the non-volatile anionic form (Lai et al., 2018;Pavlına et al., 2018). However, recent field
61 studies have confirmed their occurrence in gaseous phase (Lai et al., 2018;Cassandra et al., 2018;Ahrens et al., 2013).
62 Investigating the transport pathways of PFAAs in nationwide region via active air sampler (AAS) is challenging, due to
63 their electronic power supply and high cost. Fortunately, a number of reports showed that the XAD (a
64 styrene–divinylbenzene copolymer) impregnated sorbent based passive air sampler (SIP–PAS) and XAD based PAS
65 (XAD–PAS), were proven to be an ideal alternative sampling tool for monitoring PFAAs in a wide region, which was
66 suggested to collect a representative sample of both gas and particle phases (Lai et al., 2018;Pavlına et al., 2018).
67 XAD–PAS give PFASs profiles that were more closely resembled to those from AAS in comparing with PUF–PAS, have
68 sufficient uptake rates for the PFCAs and PFSAs to be depolyed for short time duration (Lai et al., 2018).
69 Given the factors mentioned above, we conducted a nationwide survey of PFAAs in China at a provincial level using a
70 XAD–PAS from January to December in 2017. The objective of this research was: (1) to examine the tempo–spatial
71 variations of PFAAs, and (2) to identify their potential affecting factors and evaluate the affecting pathways. To the best
72 of our knowledge, this is the first research paper analyzing both a long–term and nationwide atmospheric PFAAs data set
73 complemented by a comprehensive investigation in China.

74 **2.Material and methods**

75 **2.1 Chemicals and reagents**

76 The PFAAs standards used were Wellington Laboratories (Guelph, ON, Canada) PFAC–MXB standard materials,
77 including C5–C14 PFCAs analogues ([Perfluoropentanoic acid \(PFPeA\)](#), [Perfluorohexanoic acid \(PFHxA\)](#),
78 [Perfluoroheptanoic acid \(PFHpA\)](#), [PFOA](#), [Perfluorononanoic acid \(PFNA\)](#), [Perfluorodecanoic acid \(PFDA\)](#),
79 [Perfluoroundecanoic acid \(PFUdA\)](#), [Perfluorododecanoic acid \(PFDoA\)](#), [Perfluorotridecanoic acid \(PFTrDA\)](#), and
80 [Perfluorotetradecanoic acid \(PFTeDA\)](#)), as well as C4, C6, and C8 PFSAs analogues ([Perfluorobutane sulfonic acid](#)
81 [\(PFBS\)](#), PFHxS, and PFOS). The mass–labeled $1,2-^{13}\text{C}_2$ –PFHxA, $1,2,3,4-^{13}\text{C}_4$ –PFOA, $1,2,3,4,5-^{13}\text{C}_5$ –PFNA,
82 $1,2-^{13}\text{C}_2$ –PFDA, $1,2-^{13}\text{C}_2$ –PFUdA, $1,2-^{13}\text{C}_2$ –PFDoA, $^{18}\text{O}_2$ –PFHxS, and $1,2,3,4-^{13}\text{C}_4$ –PFOS were used as internal
83 standards (ISs, MPFAC–MXA, Wellington Laboratories Inc.) in high–performance liquid chromatography (HPLC)
84 coupled with a tandem mass spectrometer (MS/MS). HPLC–grade reagents that were used include methanol, ethyl
85 acetate, ammonia acetate, acetone, methylene dichloride, n–hexane, and Milli–Q water. Detailed sources of the target
86 PFAAs and their ISs are listed in Table S1 in the Supplementary Materials.

87 2.2 Sample collection

88 Sampling campaigns were carried out at 23 different provinces/municipalities/autonomous regions in China
89 simultaneously from January to December 2017, of which 20 were urban sites and three were rural sites (Zhejiang,
90 Shanxi, and Liaoning). Urban samples typically came from urban residential areas, and the rural samples were obtained
91 from villages. These sampling sites were divided into seven administrative divisions: norther of China (NC), southern of
92 China (SC), central of China (CC), eastern of China (EC), northwest of China (NW), northeast of China (NE), and
93 southwest of China (SW). A geographical map of the sampling sites is displayed in Figure S1, and the detailed
94 information on sampling sites such as elevation , meteorological parameters, local resident population and gross domestic
95 product were listed in Table S2.

96 Samples were collected with Amberlite XAD-2 resin using XAD-PAS, which have been successfully monitored PFCAs
97 (C4-C16) and PFSAAs (C4-C10) in the atmosphere (Krogseth et al., 2013; Armitage et al., 2013). Briefly, the mesh
98 cylinder (L.× I.D.: 10 cm × 2 cm) was prebaked at 450°C for 3 h, filled with ~10 g XAD-2 resin, and capped with an
99 aluminum cap. [The particle size of XAD-2 is ~20-60 mesh, with water content of 20%-45%, its specific surface area](#)
100 [>430 m²/g, and the reference adsorption capacity >35 mg/g. We should keep in mind that the unimpeded movement of](#)
101 [particle bound PFAAs would be captured during sampling using XAD-PAS, which cannot differentiate PFAAs between](#)
102 [gas and particle phases. Despite some research suggest the sampling efficiency of gas and particle phase PFAAs were](#)
103 [similar \(Karásková et al., 2018\). In the present study, the two phases PFAAs sampled by XAD-PAS were treated as the](#)
104 [whole atmosphere PFAAs concentration.](#) The sampling program for each sample lasted approximately a month (30 days),
105 and the error of the sampling time was controlled within 3 d. At the end of each deployment period, the atmosphere
106 samples were retrieved, resealed in their original solvent-cleaned aluminum tins at the sampling location, and transported
107 by express post to Shanghai Jiao Tong University. On receipt, they were stored and frozen ($-20\text{ }^{\circ}\text{C}$) until extraction.
108 The sampling rate of XAD-PAS is a crucial factor to derive the chemical concentrations accumulated in the XAD resin.
109 Ahrens et al. (2013) found that sampling rate of PFCAs and PFASs ranged 1.8–5.5 m³/d with XAD impregnated sorbent,
110 and the sampling rate increased as the carbon chain adding, while Karásková et al. (2018) suggested that the sampling
111 rate of XAD-PAS of 0.21–15 m³/d for PFAAs. The loss of depuration compounds could be used to calculate the
112 sampling rate, assessing the impacts from meteorological factors like temperature and wind speed. According to Ahrens
113 et al. (2013) the 1,2,3,4-¹³C₄-PFOA was used to calculate the sampling rates of PFAAs at Shanghai sampling site
114 (Shanghai Jiao Tong University) in the present study, by assessing 1,2,3,4-¹³C₄-PFOA abundance loss. The specific
115 description of the sampling rate calculation in this study is shown in Section S1 in the Supplementary Materials.

116 2.3 Sample preparation and instrument analysis

117 The sample preparation and analysis were according to the method described by previous researches (Liu et al.,
118 2015; Tian et al., 2018). The MPFAC–MXA ISs mixture surrogates (10 ng) were added to each spiked sample prior to
119 extraction. This was done to account for the loss of substances from the samples associated with instrument instability
120 caused by the changes in laboratory environmental conditions. The XAD resin samples were Soxhlet–extracted for 24 h
121 using a Soxhlet extraction system, with n–hexane: acetone (1:1, V:V) as a solvent in a 300 mL polypropylene (PP) bottle,
122 following extracted with methanol for 4 h. These two extracts were combined and reduced to ~5 mL via a rotary
123 evaporator (RE–52AA, Yarong Biochemical Instrument Inc., Shanghai, China) at a temperature below 35 °C, and then
124 transferred to a 10 mL PP tube for centrifugation (10 min, 8,000 rpm). The supernatant was transferred to another PP tube,
125 filtered three times through a 0.22 µm nylon filter, with an addition of 1 mL methanol each time. The extracts were
126 further condensed under a gentle stream of nitrogen (99.999%, Shanghai Liquid Gas Cor.) at 35 °C to a final 200 µL for
127 instrument analysis.

128 The separation and detection of PFAAs were performed using a HPLC system (Thermo Ultra 3000⁺, Thermo Scientific,
129 USA) coupled with a triple quadrupole negative electrospray ionization MS/MS (Thermo API 3000, Thermo Scientific,
130 USA). An Agilent Eclipse XDB C18 (3.5 µm, 2.1 mm, 150 mm) was used to separate the desorbed substances. The
131 column temperature was set to 40 °C, and the flow rate was 0.30 mL/min. The injection volume was 20 µL. The gradient
132 elution program of the mobile phase A (methanol) and B (5 mmol/L aqueous ammonium acetate) was 20% A + 80% B at
133 the start, 95% A + 5% B at 8 min, 100% a at 13 min, 20% A + 80% B at 14 min, and was maintained for 6 min. The
134 MS/MS was operated in a negative ion scan and multiple reaction monitoring (MRM) mode, and the electrospray voltage
135 was set to 4500 V. The ion source temperature was 450 °C. The flow rates of the atomization gas and air curtain gas was
136 10 and 9 L/min, respectively. Species identification was achieved by comparing the mass spectra and retention time of
137 the chromatographic peaks with the corresponding authentic standards.

138 2.4 Quality assurance and quality control

139 To avoid exogenous contamination, the XAD–2 resin was precleaned using a Soxhlet extraction system with acetone and
140 petroleum ether at extraction times of 24 h and 4 h, respectively. The extracted XAD resin was dried under a vacuum
141 desiccator, wrapped in an aluminum foil and zip–lock bags, and stored at –20 °C to avoid contamination. All laboratory
142 vessels were PP, and these vessels were washed with ultrapure water and methanol three times, respectively.

143 For quantification, six–point calibration curves of PFAAs were constructed by adopting different calibration solutions
144 with values of 1, 3, 6, 15, 30, and 60 ng/mL. The same concentration for the internal calibration (10 ng/mL) was used for

145 each level of the calibration solution. Recovery standards were added to each of the samples to monitor procedural
146 performance, and the mean spiked PFAAs recoveries ranged from 81%±25% to 108%±22%. All the analyzed PFAAs
147 were normalized against the recovery of the corresponding mass-labeled ISs. Field blanks were prepared at all sampling
148 sites, transported, and analyzed in the same way as the samples. Laboratory blanks were obtained by taking amounts of
149 solvent via extraction, cleanup, and analysis. A total of 8 field blanks and 26 laboratory blanks were analyzed, [with](#)
150 [individual blank values of N.D. \(not detected\)–1.1 pg/m³ and N.D.–1.3 pg/m³, respectively.](#) All the results were corrected
151 according to the blank and recovery results. The method detection limit (MDL) was derived from three times standard
152 deviation of the field blank values. The limit of detection (LOD) and the limit of quantification (LOQ) were determined
153 as a signal-to-noise ratio of 3:1 and 10:1, respectively (Rauert et al., 2018;Liu et al., 2015). To convert MDLs, LODs and
154 LOQs values to pg/m³, the mean volume of sampling air (m³) was applied. For the analytes that were not detected or
155 were below the LOQs in field blanks, MDLs were derived directly from three times the corresponding LODs. More
156 detailed information on the individual compounds of PFASs on MDL, LOD, LOQ, and the recovery values are listed in
157 Table S3.

158 **2.5 Statistical and geostatistical analysis**

159 Statistical analyses were carried out by SPSS Statistics 22 (IBM Inc. US) and SigmaPlot 14.0 (Systat Software, US). And
160 the geographical variations of atmospheric PFAAs were analyzed with ArcGIS 10.4 (ESRI, US). Positive matrix
161 factorization (PMF) is considered an advanced algorithm among various receptor models, which has been successfully
162 applied for source identification of environmental pollutants (Han et al., 2018;Han et al., 2019). PMF (5.0, US EPA) was
163 adopted to cluster the PFAAs with similar behaviors to identify potential sources, and a more detailed description of PMF
164 can be seen in Section S2.

165 **3.Results and discussion**

166 **3.1 Abundances and compositions**

167 The descriptive statistics of all targeted atmosphere PFAAs (n=268) are presented in Table 1 and Table S4. The total
168 concentrations of Σ_{13} PFAAs analogues varied between 6.19 and 292.6 pg/m³, with an average value of 39.8±28.1 pg/m³.
169 The commonly concerned PFCAs analogues (C5–C14) occupied 79.6% of the total PFAAs, at a level of 4.50–247.2
170 pg/m³, whereas the PFSAAs concentrations were 1.04–42.6 pg/m³. The long-chain PFCAs concentrations were 25.6±18.9
171 pg/m³, which were significantly higher than the short-chain (C ≤ 6) concentrations (12.3±10.9 pg/m³) (p<0.05). To the
172 contrary, a recent measurement found the long chain (C ≥ 8) PFCAs were much higher which conducted in the landfill

173 atmosphere in Tianjin, China (Tian et al., 2018). Specifically, PFOA was the dominant PFAAs (accounting 20.6%), and
 174 was detected in all atmospheric samples with an average value of $8.19 \pm 8.03 \text{ pg/m}^3$. This phenomenon could occur since
 175 PFOA is widely used in the manufacturing of polytetrafluoroethylene (PTFE), perfluorinated ethylene propolymer (FEP),
 176 and perfluoroalkoxy polymers (PFA) (Wang et al., 2014). The domestic demand for and the industrial production of
 177 PFOA-based products have been increasing in China since the late 1990s (Wang et al., 2014), and direct emissions of
 178 FOSA-based products may contribute to the relative high level of PFOA. Meanwhile, one major variation of PFOA
 179 precursor, 8:2 FTOH, was reported ranks as the highest concentration among neural PFASs in China air (De Silva,
 180 2004; Martin et al., 2006). Among PFAAs' composition profile, it was followed by PFHxA, PFOS, and PFPeA, with
 181 mean concentrations of 5.36, 5.20, and 4.95 pg/m^3 , respectively. The detection frequencies of PFCAs decreased gradually
 182 as the carbon chain length increased – for instance, the PFPeA and PFTrDA were detected in 84.8% and 37.3%,
 183 respectively.

184 Compared with other gaseous PFAAs measurements, Liu et al. (2015) reported that PFAAs in the urban atmosphere
 185 sampled with XAD-containing sorbent in Shenzhen city in China was $15 \pm 8.8 \text{ pg/m}^3$, which contributed to nearly half of
 186 this study. Wong et al. (2018) found that a much lower PFAAs levels in the remote Arctic area than this study, with mean
 187 value of 1.95 pg/m^3 . This study found generally higher PFAAs abundances compared to measurement in Canada
 188 (Gewurtz et al., 2013), which may be attributed to the relative high abundance of industrial and domestic emissions in
 189 China. However, the PFAAs concentrations in urban/rural areas in this study were far lower than the measurements at
 190 point sources, for example, landfill atmosphere (Tian et al., 2018) ($360\text{--}820 \text{ pg/m}^3$) and fluorochemical manufacturing
 191 facility (Chen et al., 2018) ($4900 \pm 4200 \text{ pg/m}^3$), suggesting that PFAAs were susceptible to being affected by local source
 192 emissions.

193

194 **Table 1.** Comparison of PFAAs levels in the present research with measurements in other areas (pg/m^3)

| Sampling sites | Duration | Sampling location | Sampler type ^a | PFAAs ^b | PFCAs ^c | Reference |
|--------------------------|-----------|--|---------------------------|--------------------------|----------------------------------|---------------------|
| 23 provinces in China | 2017.1–12 | Urban and rural areas | XAD-PAS | 6.19–292.6; 39.8±28.1 | 4.50–247.2; 31.7±23.9; C5–C14 | This study |
| Shenzhen, China | 2011.9–11 | Urban area | SIP-PAS | 3.4–34; 15±8.8 | 11.59±8.74; C4–C12 | (Liu et al., 2015) |
| Fuxin, China | 2016.9–10 | Fluorochemical manufacturing facilities | SIP-PAS | 4900±4200 | 4900±4200; C4–C12 | (Chen et al., 2018) |
| Tianjin, China | 2013 | Waste water treatment | SIP-PAS | 87.9–227; 123 | 87.9–227; 123; C6–C12 | (Yao et al., 2016a) |

| | | | | | | |
|----------------------|-------------|--------------------------|-------------------------|----------------------------|-------------------------------------|------------------------|
| | | plant | | | | |
| Tianjin, China | 2016.5–6 | Landfill | SIP-PAS | 280–820 | 280–820; C4–C12 | (Tian et al., 2018) |
| Canada | 2006–2011 | Remote and urban areas | SIP-PAS | 0.014–0.44 | 0.014–0.44; C8–C12 | (Gewurtz et al., 2013) |
| Alert, Arctic | 2006.8–2015 | Remote area | SIP-PAS | 1.95 | 1.95; C4–C8 | (Wong et al., 2018) |
| | .2 | | | | | |
| Toronto, Canada | 2010.3–10 | Semi-urban site | SIP-PAS | 11.24±7.95 | 11.24±7.95 ; C4–C18 | (Ahrens et al., 2013) |
| Brno, Czech Republic | 2013.4–9 | Suburban background site | XAD-PAS | 30–153 | 26–147.6; C4–C14 | (Pavčina et al., 2018) |

195 ^a: SIP-PAS represent XAD impregnated sorbent based PAS;

196 ^b: represent concentration range; mean value;

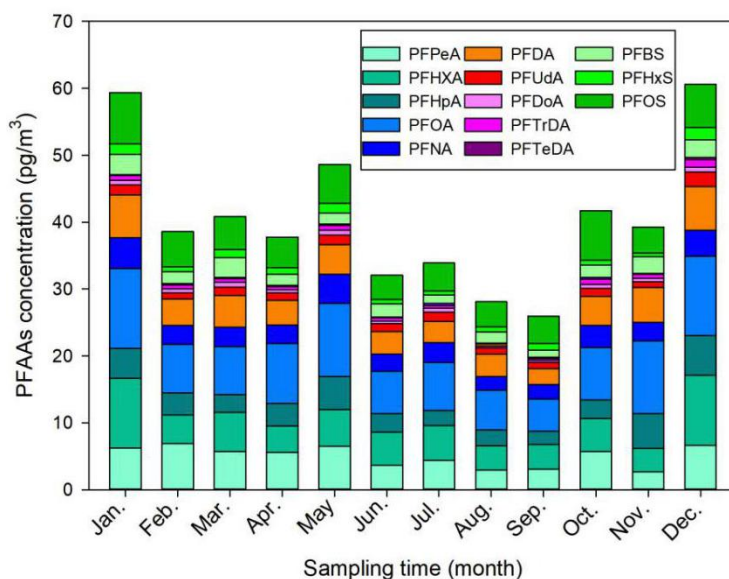
197 ^c: represent concentration range; mean value; carbon length of PFCAs.

198 3.2 Temporal variations

199 Monthly and seasonal variations of the mean PFAAs concentrations are depicted in Figure 1. In general, an increasing
200 seasonal mean of PFAAs concentrations [from 23 sampling sites](#) existed for summer (31.4 pg/m³) < autumn (35.6 pg/m³)
201 < spring (42.4 pg/m³) < winter (52.8 pg/m³). The winter maxima abundance of PFAAs may be could attribute to the
202 stagnant atmospheric conditions, in which atmospheric contaminants were trapped in the air with a weak diluting effect.
203 XAD-PAS showed similar efficiency of capturing gas and particle phases PFASs, while the unimpeded particle gathering
204 efficiency is challenging to quantify. In addition, despite the increase in atmospheric oxidation of precursors in summer
205 may lead to PFCAs rise (Li et al., 2011; Yao et al., 2016a), the abundant rainfall would enhance their scavenging activities
206 (Table S5), ultimately leading to the relatively low concentrations of PFAAs in the summer. Specifically, the PFAAs
207 showed much higher concentrations in spring than other seasons in Shanghai, which was different from Tianjin and
208 Xinjiang (Figure S2). An extreme high level of PFAAs of 135.5 pg/m³ was occurred in November in Beijing, which was
209 2–4.5 times higher than in other month, indicating the potential point source of PFAAs contamination in this site. In fact,
210 numerous fluoride related products manufacturers were distributed in EC, NC (including Beijing) and CC areas, see
211 detail in Figure S3. As gaseous PFAAs measurements were majorly reported at a relative short time (several weeks to
212 several months), it is somewhat difficult to compare their temporal trends.

213 Interestingly, the evolution of PFAAs showed a dramatic monthly variation, and the monthly mean levels varied from
214 25.9 to 60.6 pg/m³, with the lowest and the highest abundances being present in September and December, respectively.

215 For the specific composition profile of PFAAs, the average concentrations of PFOA, PFHxA, PFPeA, and PFOS were
 216 10.4, 8.42, 6.55, and 6.44 pg/m^3 in winter, respectively, which were nearly two times higher than in the summer. The
 217 seasonal variation trend of PFOS was summer < spring \approx autumn < winter, while PFNA appeared to show winter maxima
 218 with concentrations 4 and 3 times higher than in the summer and spring, respectively. However, Wong et al. (2018)
 219 reported that PFBS showed the maximal value in winter but found no consistent seasonality for PFOS in the Arctic area.
 220 The differences may be explained as the PFAAs in air in the remote Arctic area were originated from long-range
 221 transport and volatilization from snow or sea, but not affected by local direct anthropogenic emission.



222

223 **Fig. 1.** Monthly mean concentrations of PFAAs in China from January to December 2017

224

225 **3.3 Geographical distributions**

226 Due to the stark differences in topography and socioeconomic development of Chinese provinces, municipalities, or
 227 autonomous regions, as well as the enormous differences in industrialization and emissions, PFAAs showed significantly
 228 different distribution patterns in China (Figure 2). Overall, the predominant declining gradient of PFAAs' contents was
 229 CC (3 sites) > NC (3 sites) > EC (7 sites) > NE (2 sites) > SW (3 sites) > NW (3 sites) > SC (2 sites) areas in China, which
 230 was similar to previous research that the outdoor dust-bound PFAAs were relatively enriched in the eastern part of
 231 mainland China (Yao et al., 2016b). This trend was not surprising since numerous PFAAs related photoelectric industries,
 232 chemical industries, and mechanical industries are dispersed across CC, EC and NC areas, e.g., Shanghai, Zhejiang,
 233 Fujian, Henan, and Jiangsu. As expected, the western mountain and highland areas, e.g., Xinjiang and Yunnan (20.9
 234 pg/m^3), with relatively low population densities and high latitudes, displayed significantly lower PFAAs concentrations.

235 It was reported that high orographic conditions have a cold trapping effect on atmospheric PFASs, the transportation of
236 PFAAs involving particles or not should be dramatically reduced (Konstantinos et al., 2010; Yao et al., 2016a). Given that
237 altitudes increase gradually from several meters in EC, NC and SC coastal areas to nearly 2,000 meters in SW and NW
238 highland regions in China, the high altitude blocking effect for atmospheric PFAAs transportation should not be
239 neglected.

240 The annual average concentrations of PFAAs at the provincial level ranged from 12.4 pg/m³ in Xinjiang to 90.9 pg/m³ in
241 Henan, and the composition patterns varied widely. Henan contributed the largest proportion of PFAAs in China, and
242 showed the highest PFOA level (19.1 pg/m³), which is a typical, heavily-industrialized province characterized by textile
243 treatments, metal plating, and firefighting foam manufacturing, and a large amount of PFAAs emulsifier fluoropolymers
244 were used in industrial production. Special attention should be paid to Zhejiang, the level of which (61.7 pg/m³) ranked
245 second in PFAAs abundances in spite of its sampling site being located in a village. As well as this, several
246 painting-packaging plants, mechanical plants, and electrical equipment manufacturers were dispersed around this
247 sampling site (see Figure S4), which would contribute to the PFAAs variations in this site. In fact, the GDP of Zhejiang
248 ranked fourth in China, specializing in mechanical manufacture, textiles, and chemical industry. Moreover, the top six
249 sites with abundant of PFAAs were located in the most economically-developed and populated areas (the Yangtze River
250 Delta area, the Circum-Bohai Sea Region), and in the rapidly-developing regions (Henan, Sichuan) in China. In line
251 with this result, a sampling campaign conducted in Asia, including 18 sites in China, found very high levels of PFAAs
252 precursors (8:2 FTOH, 10:2 FTOH) existed in Beijing, Tianjin, and Zhejiang (Li et al., 2011). But meanwhile we should
253 keep in mind that the production of PFCAs in the atmosphere from gaseous precursors degradation may be impaired in
254 urban areas, due to the high abundance of NO_x compete for OH· radicals.

255 Furthermore, PFOA concentrations were apparently high in Henan, Zhejiang, Beijing, Tianjin, and Hubei, where mean
256 values ranged of 11.7–19.1 pg/m³ compared with in other provinces (2.93–8.54 pg/m³). PFOA and PFOA-related
257 products have not been banned for use in various industrial and domestic applications (Konstantinos et al., 2010; Wang et
258 al., 2014), which were manufactured extensively in EC and NC areas and were used widely. However, the highest
259 concentration of PFOS was found in Zhejiang (14.1 pg/m³), which may be affected by local manufacturing of PFOS
260 based products, e.g. leather, paper and metal plating. It was followed by Beijing (8.98 pg/m³) and Fujian (9.09 pg/m³),
261 while Xinjiang and Yunnan shared the lowest levels (1.20–3.57 pg/m³). This spatial variation patterns of PFOS in the
262 present study, matched well with a previous national survey that found most PFOS and its derivative facilities in China
263 are suited in EC, CC and NC areas, with emission density ranged from 1–500 g/(km²·a) (Konstantinos et al., 2010; Wang
264 et al., 2014).

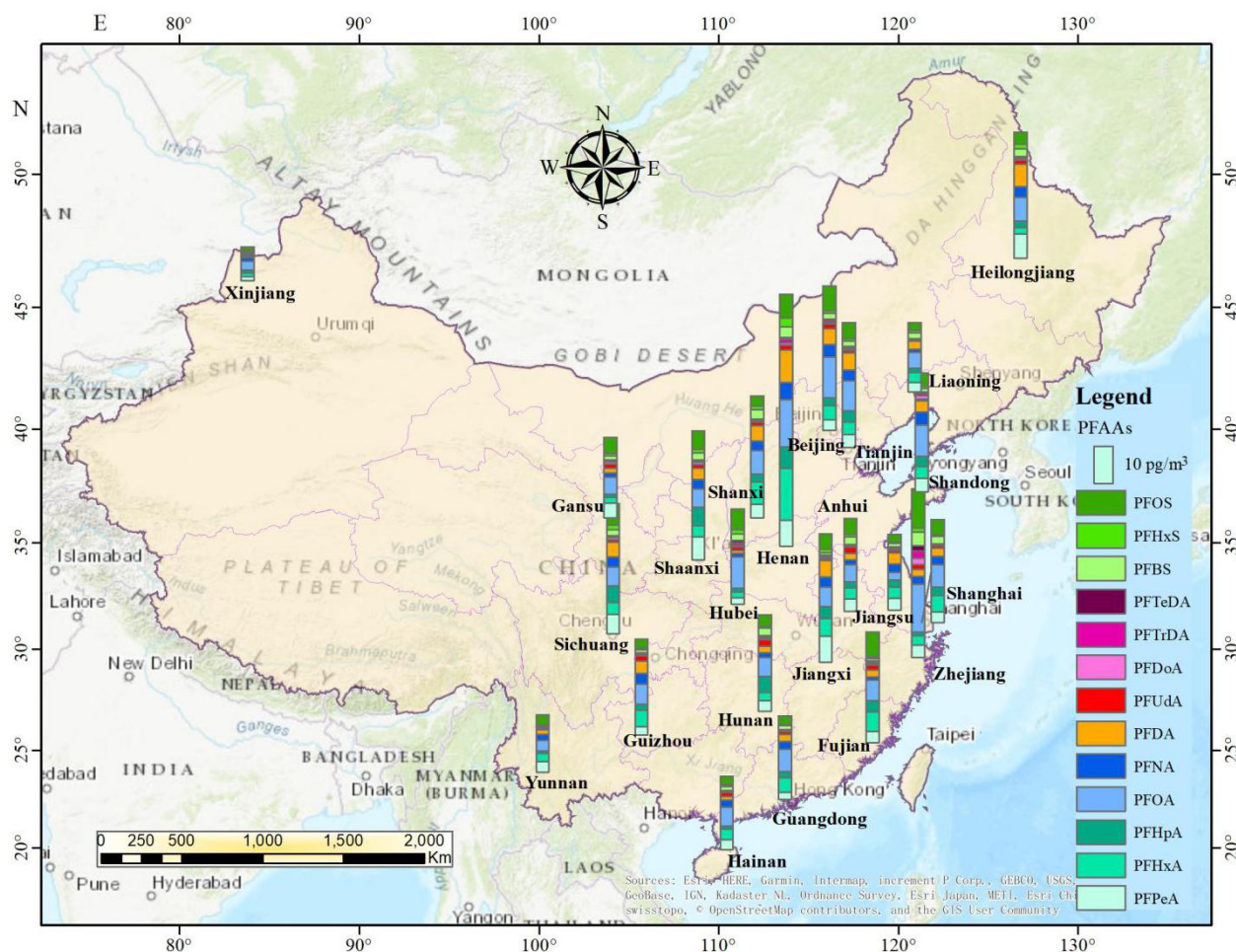


Fig. 2. The spatial distributions of PFAAs in China (annual average of PFAAs, created by ArcGIS 10.4).

3.4 Geographical distributions transport pathway

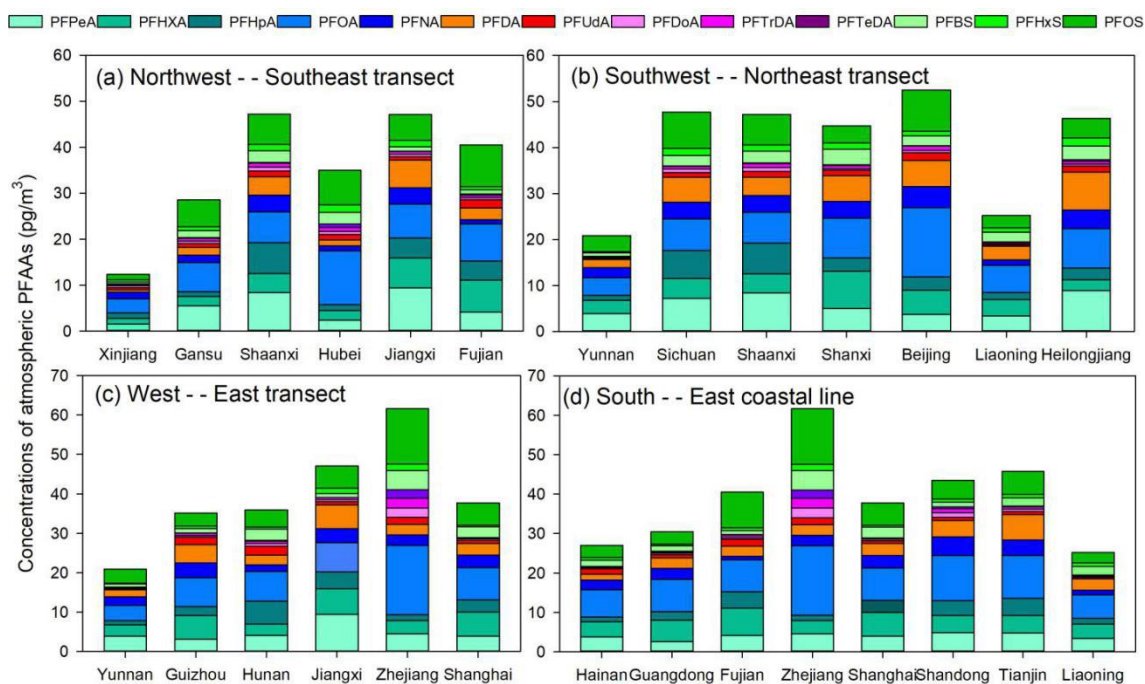
The PFAAs variations in the atmosphere depended on their local source emissions as well as regional atmosphere transportation. In order to give readers a direct impression of factors affecting the geographical variations of PFAAs in China, here we analyzed PFAAs variations along three pathway transects and one coastal line to determine how PFAAs distribute spatially.

As shown in Figure 3a, PFAAs concentrations were enriched in southeastern areas ($40.6\text{--}47.2\text{ pg/m}^3$) at low altitudes (2–30 m), but relatively low abundances ($12.3\text{--}29.4\text{ pg/m}^3$) existed in the northwestern part of China (397–1,517 m in altitude). As discussed above, the EC areas (e.g. Fujian) were the most intensively industrialized regions, direct emissions from PFAAs manufacturing processes would enhance their atmospheric abundances. However, high altitudes existed in NW areas would have a blocking effect to the transportation of PFAAs from eastern polluted areas.

In terms of the SW–NE transect (Figure 3b), Yunan and Liaoning showed much lower PFAAs concentrations (20.9 and

279 25.0 pg/m^3) than other areas (44.8–52.6 pg/m^3). Notably, a steady increasing trend of PFAAs concentrations existed
 280 across the W–E transect (Figure 3c), which escalated from 20.9 pg/m^3 in Yunnan to 61.7 pg/m^3 in Zhejiang. The
 281 composition profiles of PFAAs along this transect differed from each other; for instance, PFOA occupied 28.5% of the
 282 total PFAAs in Zhejiang, while it only accounted for 15.6%–21.8% in other areas. Note that PFAAs released from point
 283 sources would be eliminated by deposition, degradation, or dilution during transportation in the atmosphere, e.g., PFOA
 284 could decrease by 90% within 5 km of its point source (Chen et al., 2018). However, the long range transport of PFAAs
 285 bounded with particles also have been explored in previous research (Pickard et al., 2018), our Hysplit back-trajectories
 286 analysis results for Zhejiang, Jiangxi, and Shanghai confirmed that the air mass origins was a driving factor for PFAAs
 287 variation(see Figure S5).

288 Interestingly, with the exclusion of the site directly affected by surrounding sources in Zhejiang, PFAAs were rather
 289 uniformly distributed among the coastal areas, with concentrations ranging from 24.9–45.8 pg/m^3 (Figure 3d). Excluded
 290 industrial and domestic emissions as well as secondary formation, the PFAAs containing sea spray aerosols could
 291 contribute the variations of PFAAs in coastal atmosphere (Cai et al., 2012b; Pickard et al., 2018).



292
 293 **Fig. 3.** Transects of PFAAs concentrations across three different directions and one coastal line
 294

295 3.5 Source identification

296 Understanding the sources of PFAAs and their corresponding importance would enable elucidation of the levels of
 297 PFAAs in the environment. As discussed above, the observations from tempo–spatial variations of PFAAs suggest that

298 several factors may have a combined effect on the variations of PFAAs. Hence, a PMF model was adopted to extract the
299 potential factors affecting PFAAs variations, and four sources were extracted in this study (see Figure 4).

300 High percentages (~90%) of PFPeA and PFBS were found in factor 1, and were moderately loaded with PFOS (62.6%).
301 Three major types of PFOS-related chemicals; namely PFOS salts, PFOS substances and PFOS polymers, are used in
302 industrial products in China (Xie et al., 2013). PFOS salts are usually used in metal plating, firefighting foams, and
303 pesticides, while PFOS substances are adopted in paper treatment and the semiconductor industry. PFOS polymers are
304 employed for textile and leather treatment. These PFOS-related products would lead to direct emissions of PFOS during
305 their industrial and domestic activities. PFPeA and PFBS are the main substitutes for long-chain PFAAs in China, which
306 would release as impurities or by-products when manufacturing PFOS-based products (Liu et al., 2017). Hence, this
307 factor was regarded as the direct source of PFOS-based products. This was consistent with the spatial observations that
308 high PFOS concentrations were shown in Zhejiang, Fujian, Guangdong, and Shanghai, where manufacturing facilities are
309 distributed.

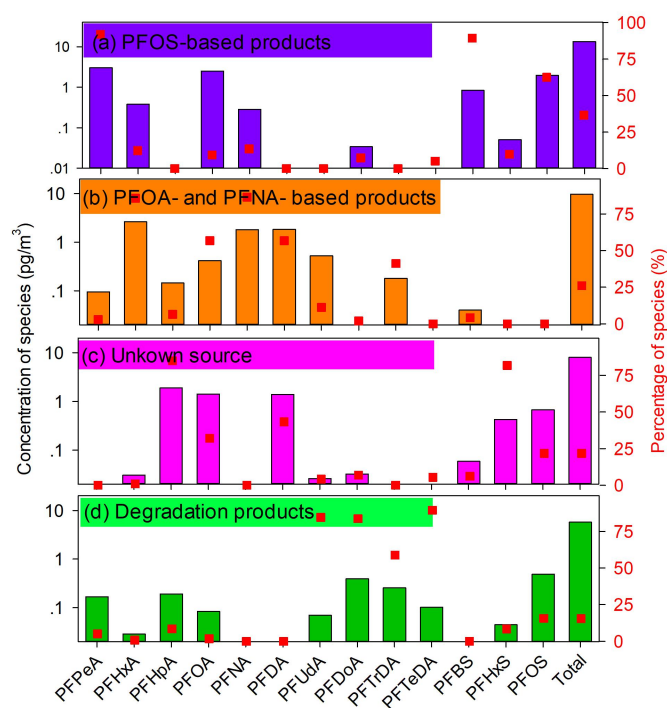
310 Factor 2 was characterized by PFHxA, PFOA, PFNA, and PFDA, each representing over 60% of their explained
311 variations. Their rather strong positive correlations ($r=0.54-0.84$, $p<0.01$) suggested that they may have originated from a
312 similar source (Table S6). PFOA was considered as the marker for the emulsification of plastics, rubber products, flame
313 retardants for textiles, paper surface treatments and fire foams (Liu et al., 2015; Konstantinos et al., 2010). It has been
314 reported that there was an increase in PFCAs emissions at the manufacturing sites of PFOA-based products in China
315 between 2002 and 2012 due to a rapid increase in domestic demand and production of PFOA-related products (Wang et
316 al., 2014). PFNA and its derivatives have similar physicochemical properties to PFOA and its derivatives, and both can
317 be emitted through exhaust gases. The PFNA-based production was found to be related to polyvinylidene fluoride
318 (PVDF) production, and it has been suggested that PVDF production increased in China after 2008 (Wang et al., 2014).
319 Therefore, factor 2 represents direct sources of PFOA-based and PFNA-based products.

320 The compositions of factor 3 were characterized by a high loading of PFHpA and PFHxS, with loading factor values of
321 84.9% and 81.7%, respectively. The historical production and uses of PFHpA and its derivatives remain unidentified.
322 Factor with PFHxS alone did not indicate a specific source, so this factor may be classified as an unknown source, which
323 may be affected by atmosphere air mass transport, sea aerosol bursting and/or other origins.

324 The final factor was dominated by PFUdA, PFDaA, PFTrDA, and PFTeDA, with loading factor values larger than 80%.
325 These long-chain PFAAs (C11-C14) analogues have been interpreted as degradation products of fluorotelomer-based
326 products in previous research (Liu et al., 2017; Wang et al., 2014; Thackray and Selin, 2017). Based on the life-cycle
327 usage and release from fluorotelomer and other fluorinated products, the global cumulative estimation of PFUdA,

328 PFDoA, PFTrDA, and PFTeDA from quantified sources was estimated to be 9–230 tons in the period of 2003–2015, and
 329 projected to be between 0–84 tons between 2016–2030 (Wang et al., 2014). It was reported that the manufacturing of
 330 fluorotelomer-based substances would increase in China. In addition, these four analogues showed apparent positive
 331 correlations each other ($r = 0.59-0.79$, $p < 0.01$). Thus, this factor was explained as the degradation products of
 332 fluorotelomer-based products, which could be proven by their higher abundances caused by an enhanced atmospheric
 333 oxidation ability in the summer than other seasons.

334 Direct emission sources, including PFOS-based products, PFOA-based products, and PFNA-based products were
 335 estimated to represent 62.7% of the total PFAAs sources. Indirect sources of degradation products of
 336 fluorotelomer-based products played a minor role, contributing 15.5%, and there are 21.8% of variances that could still
 337 not be explained and need further detailed investigation. This source apportionment result was similar to one recent piece
 338 of research that found that industrial PFOA emissions were the major sources of atmospheric PFAAs in Shenzhen, China
 339 (Liu et al., 2015), and the long-distance transportation of pollutants also made a contribution.



340
 341 **Fig. 4.** Factor profiles of PFAAs extracted by the PMF model

342 **4. Conclusion**

343 In the present study, PFAAs were ubiquitously detected in the atmosphere across China over the length of a year. Results
 344 indicated that the measured PFAAs were several times to several magnitudes higher than other urban atmosphere levels,

345 and much higher abundances existed in winter seasons compared with in the summer. In terms of spatial distribution, the
346 PFAAs concentrations were higher in central and eastern China, where dense residential and industrial manufacturing
347 facilities were distributed. Correlation, Hysplit backward trajectories, and a PMF receptor model suggested that the direct
348 sources of PFOS-based, PFOA-based, and PFNA-based products made a predominant contribution to variations in
349 PFAAs, while indirect degradation played a minor role.

350 **Acknowledgements**

351 This study was financially supported by National Key Research & Development Plan (2016YFC0200104), National
352 Natural Science Foundation of China (No. 21577090 and No. 21777094), and China Postdoctoral Innovative Talent
353 Support Project (BX20190169). We thank Lei Ye (Xi'an University of Architecture and Technology), Fengxia Wang
354 (Hainan University), Linrui Jia (Beijing Normal University), Songfeng Chu (Tongji University), and other 18 volunteers,
355 for coordinating the sampling process and for their valuable contribution to field measurement. We appreciate senior
356 engineer Xiaofang Hu (Instrumental Analysis Center, SESE, Shanghai Jiao Tong University) for her assistance in
357 experiment analysis.

358 **Appendix A: Supplementary material**

359 **References**

- 360 Ahrens, L., Harner, T., Shoeib, M., Koblizkova, M., and Reiner, E. J.: Characterization of Two Passive Air Samplers for
361 Per- and Polyfluoroalkyl Substances, *Environ. Sci. Technol.*, 47, 14024-14033, <https://doi.org/10.1021/es4048945>, 2013.
- 362 Armitage, J. M., Hayward, S. J., and Frank, W.: Modeling the Uptake of Neutral Organic Chemicals on XAD Passive Air
363 Samplers under Variable Temperatures, External Wind Speeds and Ambient Air Concentrations (PAS-SIM), *Environ. Sci.*
364 *Technol.*, 47, 13546-13554, <https://doi.org/10.1021/es402978a>, 2013.
- 365 Baard Ingegerdsson, F., Line Sm. Stuen, H., Raymond, O., Hanne Line, D., Merete, H., Cathrine, T., Syvert, T., Georg, B.,
366 Paal, M., and Ellingsen, D. G.: Occupational exposure to airborne perfluorinated compounds during professional ski
367 waxing, *Environ. Sci. Technol.*, 44, 7723-7728, <https://doi.org/10.1021/es102033k>, 2010.
- 368 Cai, M., Xie, Z., Moeller, A., Yin, Z., Huang, P., Cai, M., Cai M. Yang, H., Sturm, R., and He, J.: Polyfluorinated
369 compounds in the atmosphere along a cruise pathway from the Japan Sea to the Arctic Ocean, *Chemosphere*, 87(9),
370 989-997 <https://doi.org/10.1016/j.chemosphere.2011.11.010>, 2012a.

371 Cai M., Zheo, Z., Yin Z., Ahrens L., Huang P., Cai M., Yang H., He J., Sturm R., Ebinghaus R., Xie Z.: Occurrence of
372 perfluoroalkyl compounds in surface waters from the North Pacific to the Arctic Ocean, *Environ. Sci. Technol.*, 46,
373 661-668, <https://doi.org/10.1021/es2026278>, 2012b.

374 Cardenas, A., Gold, D. R., Hauser, R., Kleinman, K. P., Hivert, M. F., Calafat, A. M., Ye, X., Webster, T. F., Horton, E. S.,
375 and Oken, E.: Plasma Concentrations of Per- and Polyfluoroalkyl Substances at Baseline and Associations with Glycemic
376 Indicators and Diabetes Incidence among High-Risk Adults in the Diabetes Prevention Program Trial, *Environ Health*
377 *Perspect*, 125, 107001, <https://doi.org/10.1289/EHP1612>, 2017.

378 Cassandra, R., Tom, H., K, S. J., Anita, E., Gilberto, F., Eugenia, C. L., Oscar, F., Martin, V. I., S.B., M. K., and Isabel, M.
379 R.: Atmospheric concentrations of new POPs and emerging chemicals of concern in the Group of Latin America and
380 Caribbean (GRULAC) region, *Environ. Sci. Technol.*, 52(13), 7240-7249, <https://doi.org/10.1021/acs.est.8b00995>, 2018.

381 Chen, H., Yao, Y., Zhao, Z., Wang, Y., Wang, Q., Ren, C., Wang, B., Sun, H., Alder, A. C., and Kannan, K.: Multimedia
382 Distribution and Transfer of Per- and Polyfluoroalkyl Substances (PFASs) Surrounding Two Fluorochemical
383 Manufacturing Facilities in Fuxin, China, *Environ. Sci. Technol.*, 52, 8263-8271, <https://doi.org/10.1021/acs.est.8b00544>,
384 2018.

385 De Silva, A. O.: Degradation of fluorotelomer alcohols: a likely atmospheric source of perfluorinated carboxylic acids,
386 *Environ. Sci. Technol.*, 38, 3316-33121, <https://doi.org/10.1021/es049860w>, 2004.

387 Dreyer, A., Weinberg, I., Temme, C., and Ebinghaus, R.: Polyfluorinated Compounds in the Atmosphere of the Atlantic
388 and Southern Oceans: Evidence for a Global Distribution, *Environ. Sci. Technol.*, 43, 6507-6514, [https://doi.org/](https://doi.org/10.1021/es9010465)
389 [10.1021/es9010465](https://doi.org/10.1021/es9010465), 2009.

390 Gewurtz, S. B., Backus, S. M., Silva, A. O., De, Lutz, A., Alain, A., Marlene, E., Susan, F., Melissa, G., Paula, G., and
391 Tom, H.: Perfluoroalkyl acids in the Canadian environment: multi-media assessment of current status and trends, *Environ.*
392 *Int.*, 59, 183-200, <https://doi.org/10.1016/j.envint.2013.05.008>, 2013.

393 Han, D., Fu, Q., Gao, S., Li, L., Ma, Y., Qiao, L., Xu, H., Liang, S., Cheng, P., Chen, X., Zhou, Y., Yu, J. Z., and Cheng,
394 J.: Non-polar organic compounds in autumn and winter aerosols in a typical city of eastern China: size distribution and
395 impact of gas-particle partitioning on PM2.5 source apportionment, *Atmos. Chem. Phys.*, 18, 9375-9391, [https://doi.org/](https://doi.org/10.5194/acp-18-9375-2018)
396 [10.5194/acp-18-9375-2018](https://doi.org/10.5194/acp-18-9375-2018), 2018.

397 Han, D., Fu, Q., Gao, S., Zhang, X., Feng, J., Chen, X., Huang, X., Liao, H., Cheng, J., and Wang, W.: Investigate the
398 impact of local iron-steel industrial emission on atmospheric mercury concentration in Yangtze River Delta, China,
399 *Environ. Sci. Pollut. Res.*, 26(6), 5862-5872, <https://doi.org/10.1007/s11356-018-3978-7>, 2019.

400 Hu, X. C., Andrews, D. Q., and Lindstrom, A. B.: Detection of Poly- and Perfluoroalkyl Substances (PFASs) in U.S.

401 Drinking Water Linked to Industrial Sites, Military Fire Training Areas, and Wastewater Treatment Plants, *Environ. Sci.*
402 *Technol. Lett.*, 3, 344-350, <https://doi.org/10.1021/acs.estlett.6b00260>, 2016.

403 Jian, J. M., Guo, Y., Zeng, L., Liu, L. Y., Lu, X., Wang, F., and Zeng, E. Y.: Global distribution of perfluorochemicals
404 (PFCs) in potential human exposure source—A review, *Environ. Int.*, 108, 51-62, <https://doi.org/>, 2017.

405 Johansson, N., Fredriksson, A., and Eriksson, P.: Neonatal exposure to perfluorooctane sulfonate (PFOS) and
406 perfluorooctanoic acid (PFOA) causes neurobehavioural defects in adult mice, *Neurotoxicology*, 29, 160-169,
407 <https://doi.org/10.1016/j.neuro.2007.10.008>, 2008.

408 Karásková, P., Codling, G., Melymuk, L., and Klánová, J.: A critical assessment of passive air samplers for per- and
409 polyfluoroalkyl substances, *Atmos. Environ.*, 185, 186-195, <https://doi.org/10.1016/j.atmosenv.2018.05.030>, 2018.

410 Konstantinos, P., Cousins, I. T., Buck, R. C., and Korzeniowski, S. H.: Sources, fate and transport of
411 perfluorocarboxylates, *Environ. Sci. Technol.*, 40(1), 32-44, <https://doi.org/10.1002/chin.200611255>, 2010.

412 Krogseth, I. S., Xianming, Z., Ying, D., Lei, Frank, W., and Knut, B.: Calibration and application of a passive air sampler
413 (XAD-PAS) for volatile methyl siloxanes, *Environ. Sci. Technol.*, 47, 4463-4470, <https://doi.org/10.1021/es400427h>,
414 2013.

415 Lai, F. Y., Rauert, C., Gobelius, L., and Ahrens, L.: A critical review on passive sampling in air and water for per- and
416 polyfluoroalkyl substances (PFASs), *TrAC Trends Anal. Chem.*, Available online 23 Nov. 2018, [https://doi.org/](https://doi.org/10.1016/j.trac.2018.11.009)
417 [10.1016/j.trac.2018.11.009](https://doi.org/10.1016/j.trac.2018.11.009), 2018.

418 Li, J., Vento, S. D., Schuster, J., Gan, Z., Chakraborty, P., Kobara, Y., and Jones, K. C.: Perfluorinated Compounds in the
419 Asian Atmosphere, *Environ. Sci. Technol.*, 45, 7241-7428, <https://doi.org/10.1021/es201739t>, 2011.

420 Lindstrom, A. B., Strynar, M. J., and Libelo, E. L.: Polyfluorinated Compounds: Past, Present, and Future, *Environ. Sci.*
421 *Technol.*, 45, 7954-7961, <https://doi.org/10.1021/es2011622>, 2011.

422 Liu, B., Zhang, H., Yao, D., Li, J., Xie, L., Wang, X., Wang, Y., Liu, G., and Yang, B.: Perfluorinated compounds (PFCs)
423 in the atmosphere of Shenzhen, China: Spatial distribution, sources and health risk assessment, *Chemosphere*, 138,
424 511-518, <https://doi.org/10.1016/j.chemosphere.2015.07.012>, 2015.

425 Liu, Z., Lu, Y., Wang, P., Wang, T., Liu, S., Johnson, A. C., Sweetman, A. J., and Baninla, Y.: Pollution pathways and
426 release estimation of perfluorooctane sulfonate (PFOS) and perfluorooctanoic acid (PFOA) in central and eastern China,
427 *Sci. Total Environ.*, 580, 1247-1256, <https://doi.org/10.1016/j.scitotenv.2016.12.085>, 2017.

428 Martin, J. W., Ellis, D. A., Mabury, S. A., Hurley, M. D., and Wallington, T. J.: Atmospheric chemistry of
429 perfluoroalkanesulfonamides: kinetic and product studies of the OH radical and Cl atom initiated oxidation of N-ethyl
430 perfluorobutanesulfonamide, *Environ. Sci. Technol.*, 40, 864-872, <https://doi.org/10.1021/es051362f>, 2006.

431 Pavlína, K., Garry, C., Lisa, M., and Jana, K.: A critical assessment of passive air samplers for per- and polyfluoroalkyl
432 substances, *Atmos. Environ.*, 185, 186-195, <https://doi.org/10.1016/j.atmosenv.2018.05.030>, 2018.

433 Pickard H. M., Criscitiello A. S., Spencer C., Sharp M. J., Muir D.C. G., De Silva A. O., Young C. J.: Continuous
434 non-marine inputs of per- and polyfluoroalkyl substances to the High Arctic: a multi-decadal temporal record, *Atmos.*
435 *Chem. Phys.*, 18, 5045–5058, <https://doi.org/10.5194/acp-18-5045-2018>, 2018.

436 Rauert, C., Harner, T., Schuster, J. K., Eng, A., Fillmann, G., Castillo, L. E., Fentanes, O., Villa, M. I., Miglioranza, K.,
437 and Moreno, I. R.: Atmospheric Concentrations of New Persistent Organic Pollutants and Emerging Chemicals of
438 Concern in the Group of Latin America and Caribbean (GRULAC) Region, *Environ. Sci. Technol.*, 52(13), 7240-7249,
439 <https://doi.org/10.1021/acs.est.8b00995>, 2018.

440 Sedlak, M. D., Benskin, J. P., Wong, A., Grace, R., and Greig, D. J.: Per- and polyfluoroalkyl substances (PFASs) in San
441 Francisco Bay wildlife: Temporal trends, exposure pathways, and notable presence of precursor compounds,
442 *Chemosphere*, 185, 1217-1226, <https://doi.org/10.1016/j.chemosphere.2017.04.096>, 2017.

443 Thackray, C. P., Selin N. E.: Uncertainty and variability in atmospheric formation of PFCAs from fluorotelomer
444 precursors, *Atmos. Chem. Phys.*, 17, 4585–4597, <https://doi.org/10.5194/acp-17-4585-2017>, 2017.

445 Tian, Y., Yao, Y., Chang, S., Zhao, Z., Zhao, Y., Yuan, X., Wu, F., and Sun, H.: Occurrence and Phase Distribution of
446 Neutral and Ionizable Per- and Polyfluoroalkyl Substances (PFASs) in the Atmosphere and Plant Leaves around Landfills:
447 A Case Study in Tianjin, China, *Environ. Sci. Technol.*, 52, 1301-1310, <https://doi.org/10.1021/acs.est.7b05385>, 2018.

448 Tian, Y., Zhou, Y., Miao, M., Wang, Z., Yuan, W., Liu, X., Wang, X., Wang, Z., Wen, S., and Liang, H.: Determinants of
449 plasma concentrations of perfluoroalkyl and polyfluoroalkyl substances in pregnant women from a birth cohort in
450 Shanghai, China, *Environment International*, 119, 165-173, <https://doi.org/10.1016/j.envint.2018.06.015>, 2018.

451 Wang, Q. W., Yang, G. P., Zhang, Z. M., and Jian, S.: Perfluoroalkyl acids in surface sediments of the East China Sea,
452 *Environ. Pollut.*, 231, 59-67, <https://doi.org/10.1016/j.envpol.2017.07.078>, 2017.

453 Wang, Z., Cousins, I. T., Scheringer, M., Buck, R. C., and Hungerbühler, K.: Global emission inventories for C4-C14
454 perfluoroalkyl carboxylic acid (PFCA) homologues from 1951 to 2030, Part I: production and emissions from
455 quantifiable sources, *Environ. Int.*, 70, 62–75, <https://doi.org/10.1016/j.envint.2014.04.013>, 2014.

456 Wang X., Schuster J., Jones K. C., Gong P.: Occurrence and spatial distribution of neutral perfluoroalkyl substances and
457 cyclic volatile methylsiloxanes in the atmosphere of the Tibetan Plateau, *Atmos. Chem. Phys.*, 18, 8745–8755,
458 <https://doi.org/10.5194/acp-18-8745-2018>, 2018.

459 Wong, F., Shoeib, M., Katsoyiannis, A., Eckhardt, S., Stohl, A., Bohlinizzetto, P., Li, H., Fellin, P., Su, Y., and Hung, H.:
460 Assessing temporal trends and source regions of per- and polyfluoroalkyl substances (PFASs) in air under the Arctic

461 Monitoring and Assessment Programme (AMAP), *Atmos. Environ.*, 172, 65-73, [https://doi.org/](https://doi.org/10.1016/j.atmosenv.2017.10.028)
462 10.1016/j.atmosenv.2017.10.028, 2018.

463 Xie, S., Wang, T., Liu, S., Jones, K. C., Sweetman, A. J., and Lu, Y.: Industrial source identification and emission
464 estimation of perfluorooctane sulfonate in China, *Environ. Int.*, 52, 1-8, <https://doi.org/10.1016/j.envint.2012.11.004>,
465 2013.

466 Yao, Y., Chang, S., Sun, H., Gan, Z., Hu, H., Zhao, Y., and Zhang, Y.: Neutral and ionic per- and polyfluoroalkyl
467 substances (PFASs) in atmospheric and dry deposition samples over a source region (Tianjin, China), *Environ Pollut*, 212,
468 449-456, <https://doi.org/10.1016/j.envpol.2016.02.023>, 2016a.

469 Yao, Y., Sun, H., Gan, Z., Hu, H., Zhao, Y., Chang, S., and Zhou, Q. X.: A Nationwide Distribution of Per- and
470 Polyfluoroalkyl Substances (PFASs) in Outdoor Dust in Mainland China From Eastern to Western Areas, *Environ. Sci.*
471 *Technol.*, 50(7), 3676-3685, <https://doi.org/10.1021/acs.est.6b00649>, 2016b.